Available online at www.sciencedirect.com
ScienceDirect
Journal of the European Ceramic Society 26 (2006) 3567–3574
www.elsevier.com/locate/jeurceramsoc

Thermal conductivity of highly porous zirconia

B. Nait-Ali [a], K. Haberko [b], H. Vesteghem [a], J. Absi [a], D.S. Smith [a,*]

[a] *Groupe d'Etude des Matériaux Hétérogènes, Ecole Nationale Supérieure de Céramique Industrielle, 47 à 73, Avenue Albert Thomas 87065 Limoges Cedex, France*

[b] *University of Mining and Metallurgy, Faculty of Materials Science and Ceramics, Al. Mickiewicza 30, 30-059 Krakow, Poland*

Received 14 April 2005; received in revised form 27 October 2005; accepted 19 November 2005
Available online 18 January 2006

Abstract

Highly porous zirconia ceramic with nanometric sized grains was prepared from an 8 mol% yttria stabilised zirconia suspension mixed with a commercial latex. The pore volume fraction was varied from 45 to 75% by adjusting the thermal treatment between 750 and 1100 °C. Observations of the microstructure reveal variation in pore shape and size. Mean grain sizes are less than 70 nm. Mercury porosimetry measurements reveal a bimodal pore size distribution. Thermal diffusivity measurements were made with the laser flash technique in order to determine the thermal conductivity at room temperature. The thermal conductivity approaches a lower limit of 0.1 $W m^{-1} K^{-1}$. Experimental results were shown to agree closely with predictions made with Landauer's effective medium expression for a two-phase system. The agreement was improved even further by taking into account the interfacial thermal resistance of the grain boundaries and the pore size distribution.

Keywords: Thermal conductivity; Porosity; ZrO_2; Analytical models

1. Introduction

Research towards a better understanding of the physical properties of heterogeneous solids has both scientific and technological importance. One particular class of these solids is constituted by materials containing a large volume fraction of porosity which are used in situations requiring very good thermal insulation, typically at high temperatures. Refractory materials for thermal insulation can be classified by the amount of porosity: lightweight material with a total porosity from 45 to 75%, extremely lightweight material from 75 to 85% and ultra-lightweight material with porosity exceeding 85%[1].

Fibrous insulating materials are ultra-lightweight and exhibit low thermal conductivity from 0.3 $W m^{-1} K^{-1}$ to less than 0.1 $W m^{-1} K^{-1}$. The European Ceramic Fibre Industries Association (ECFIA) has established a classification of man-made vitreous silicate fibres with the corresponding health and safety regulations[2]. This classification has led to the following conclusion: the use of fibrous insulating materials should be reviewed for each application and possible substitutes considered. According to the report, future research should be devoted to the thermal conductivity of ceramics containing pore volume fractions above 45%.

In earlier work, we have demonstrated the decrease of effective thermal conductivity due to grain boundary thermal resistance for the case of small grain alumina ceramics containing up to 30% porosity[3]. The present contribution examines the influence of the pore volume fraction and other microstructural factors on the effective thermal conductivity of stabilized zerconia, for pore volume fractions between 45 and 73% (lightweight materials). Both experimental measurements and analytical calculations have been made. A stabilized zirconia matrix has been chosen for several reasons. First, it has a low intrinsic thermal conductivity close to 2 $W m^{-1} K^{-1}$ which reduces the relative effect of the grain boundary thermal resistance. Second, stabilized zirconia is used in insulating applications such as thermal barrier coatings. Finally, stabilized zirconia has been widely investigated and much useful data can be found in the literature.

An analytical model can be used to predict the effective thermal conductivity of the porous material providing a value for the thermal conductivity of the solid phase is known. Many analytical expressions exist which relate transport phenomena in two-phase systems to the properties of each phase, the microstructure and the volume fractions. Since, in the porosity range of our samples, the different expressions can give significant variation in

* Corresponding author. Tel.: +33 55 5452222; fax: +33 55 5790998.
E-mail address: d_smith@ensci.fr (D.S. Smith).

0955-2219/$ – see front matter © 2005 Elsevier Ltd. All rights reserved.
doi:10.1016/j.jeurceramsoc.2005.11.011

the predicted values depending on the geometrical simplifications implied, a brief review of analytical models is made in Section 3 in order to explain the particular choice of Landauer's effective medium expression. The basic two-phase model uses as input parameters thermal conductivity and pore volume fraction of each phase. The calculations are further refined, to include in a simple way detailed microstructural information such as grain boundary density in the heat path and pore size distribution. These second order effects are shown to be relevant to the interpretation of experimental results.

2. Experimental procedure

2.1. Sample preparation

A hydrothermally crystallized 8 mol% yttria stabilised zirconia (8-YSZ) suspension, prepared in the University of Science and Technology of Krakow (Poland)[4], was mixed with a commercial latex. Transmission Electron Microscope (TEM) observation in Fig. 1 shows a crystallite size of about 6 nm. The specific surface area of the powder is 169 $m^2\,g^{-1}$. Crystallites form agglomerates with a mean grain size of about 1 μm. The latex Rhoximat UP 600B from the Rhodia Company was used with a volume ratio with respect to the solid content: $V_{\text{solid polymer}}/V_{\text{total solid}} = 0.7$. The mean particle size of the polymer depends on the dilution and its value is between 1 and 5 μm.

After drying the mixture for 24 h at room temperature in order to form a paste, disk samples were uniaxially pressed at 100 MPa. This was followed by a thermal treatment as defined in Fig. 2. The organic additive was burned out at the end of the first stage. The pore volume fraction was varied from 45 to 75% by adjusting the thermal treatment between 750 and 1100 °C. Fig. 3 shows the dilatometric curve of a sample which was previously fired at 600 °C for 1 h. The shrinkage becomes significant above 900 °C. This curve was used to choose the different maximum temperatures $T_{\max}$ of the firing cycle.

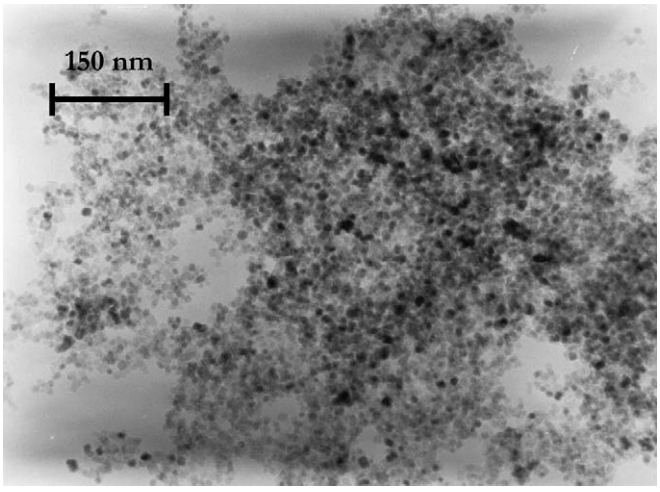

Fig. 1. TEM observation of ZrO_2 8 mol% Y_2O_3 crystallites.

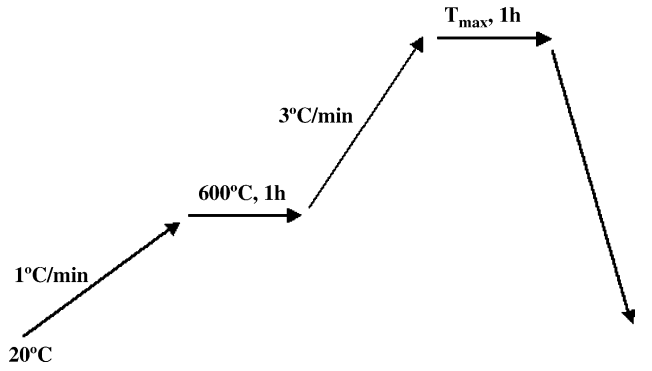

Fig. 2. Thermal treatment of zirconia samples after uniaxial pressing at 100 MPa.

2.2. Microstructure characterisation

The pore volume fraction in each sample was determined by the method based on the Archimedes' principle. The calculation requires knowledge of the solid phase density. A literature value[5] determined by the X-ray diffraction measurement of the 8-YSZ lattice parameter was used: 6.033 g cm^{-3}.

Our interest was focused on the characterisation of the porous network. Fractures of samples were observed by scanning electron microscope (SEM). These micrographs give information about grain sizes, pore shape and size. Mean grain sizes were evaluated from micrographs using image analysis software. The pore size distributions in the samples were also evaluated using mercury porosimetry measurements.

2.3. Thermal conductivity measurement

The flash method was used to determine, via the thermal diffusivity, the effective thermal conductivity of the samples[6]. The flash source is a neodymium-glass laser operating at 1.053 μm. This laser which delivers a standard pulse of 30 J in 450 μs was used to heat up the front face of the cylindrical sample. The absorbed heat diffuses throughout the sample and a liquid-nitrogen-cooled infra-red detector (Hg-Cd-Te) was used to monitor the evolution of the back face temperature. Because Zirconia is semi-transparent to near infrared wavelengths, samples were coated with a thin graphite layer in order to avoid

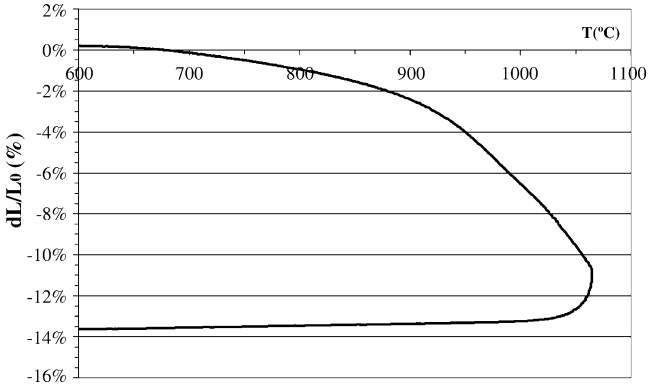

Fig. 3. Shrinkage of zirconia bar, previously fired at 600 °C for 1 h, as a function of temperature for a heating ramp of 1 °C/min.

the propagation of the laser radiation through the thickness of the material. This also improves the laser beam absorption and the emitted signal of the back face. Typical dimensions of the disk samples were 2 mm in thickness and 10 mm in diameter. Measurements were performed in air which corresponds to the general service condition for insulating materials. Degiovanni's method, which takes into account heat losses, was used to calculate the thermal diffusivity (α) from an analysis of the back face temperature–time behaviour[7]. Assuming the sample behaves as a homogeneous medium, the thermal conductivity is then obtained with the expression:

$$\lambda = \alpha \times \rho \times c \tag{1}$$

where ρ is the density and c is the specific heat of the material. The specific heat was obtained from literature values which take into account the molar fraction of Y_2O_3 in the zirconia matrix[8].

3. Effective thermal conductivity of porous solids: analytical expressions

A porous solid can be assimilated to a two-phase system constituted by a dense solid skeleton and air. The effective thermal conductivity describes heat transfer through this complex system. Collishaw[9] has reviewed some of expressions for the calculation of the effective thermal conductivity of a porous solid. In each case, the expression is based on a geometrical simplification of the microstructure concerning the spatial distribution of the pore phase in the solid matrix. The pertinence of this approximation to the real microstructure determines the validity of a chosen model.

We can consider two groups of expressions according to the assumptions which are made to describe the nature of the microstructure. The first group, constituted by asymmetrical models, concerns the dispersion of a second phase in a continuous matrix. Maxwell[10], Rayleigh[11] and Russel[12] propose expressions for, respectively, spherical, cylindrical, and cubic inclusions dispersed in the matrix. The Hashin and Shtrikman expressions, Eqs. (2) and (3), give the most restrictive upper and lower limits of the effective thermal conductivity for a two-phase system where spherical inclusions are placed in a continuous matrix[13](Fig. 4a and b). The upper limit simply corresponds to the Maxwell calculation[10].

$$\lambda_{\text{eff,min}} = \lambda_s + \frac{v_p}{1/(\lambda_p - \lambda_s) + (v_s/3\lambda_s)} \tag{2}$$

$$\lambda_{\text{eff,max}} = \lambda_p + \frac{v_s}{1/(\lambda_s - \lambda_p) + (v_p/3\lambda_s)} \tag{3}$$

λ_s and λ_p are the thermal conductivities of, respectively, the solid matrix and the pores, v_s and v_p are the corresponding volume fractions of these phases. λ_{eff} is the effective thermal conductivity.

The expressions in the second group, or symmetrical models, take into account a more continuous nature to the second phase. Bruggeman[14] has proposed an equation which can be applied to calculation of the effective thermal conductivity of two interconnected phases and uses the concept of an "effective medium". In this approach, the two phases play interchangeable roles which justify the name of symmetrical model. A random mixture of spherical particles of the two different phases is considered (Fig. 4c). The neighbourhood of each such particle is assumed to exhibit the thermal conductivity which characterizes the mixture. Each phase exhibits a more or less continuous nature depending on its volume fraction. Landauer[15] derived a practical expression, Eq. (4), corresponding, in fact, to the solution of Bruggeman's equation and this is used extensively in the present paper. This approach is also called "Effective Medium Percolation Theory" (EMPT)[16].

$$\lambda_{\text{eff}} = \frac{1}{4}[\lambda_p(3v_p - 1) + \lambda_s(3v_s - 1) + ([\lambda_p(3v_p - 1) + \lambda_s(3v_s - 1)]^2 + 8\lambda_p\lambda_s)^{1/2}] \tag{4}$$

Finally, we mention the approach where the shape and orientation of the pores with respect to the heat flow are taken into account. Schulz[17] has developed an expression for isolated inclusions which includes factors for the ellipsoid shape of the pore and also its orientation. In a similar vein, Bjorneklett et al. have extended the Bruggeman approach to treat the case for more or less interconnected ellipsoids[18]. This last model is particularly relevant to plasma sprayed thermal barrier coatings where the pores are shaped as thin lamellae and oriented perpendicularly to the heat flow direction.

For materials containing small amounts of porosity (<20%), the choice of an analytical model is less critical than for highly porous materials. Indeed the values calculated from analytical models presented here, only start to diverge strongly for porosity exceeding 20%. Obviously for materials which exhibit open porosities, analytical theory based on dispersed inclusions is of restricted use. The choice of an analytical model has to take into

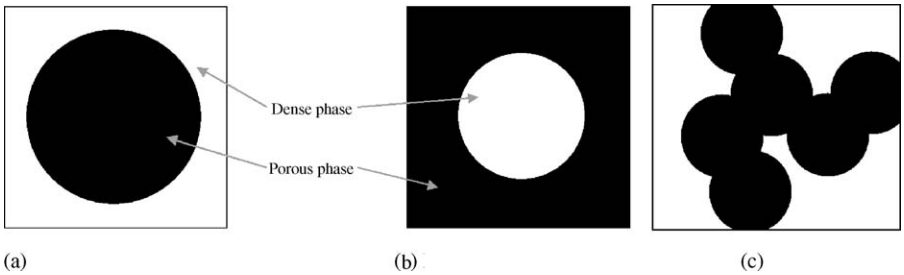

Fig. 4. Schematic representations of microstructures used in analytical models. (a) Hashin Shtrikman Upper limit HS+. (b) Hashin Shtrikman Lower limit HS−. (c) EMPT.

Table 1
Pore volume fraction as a function of the maximum temperature used in the firing cycle, T_{max}

T_{max} (°C)	Apparent density (kg m^{-3})	Porosity (%)
750	1653	73
850	1713	72
950	1943	68
1000	2274	62
1040	2576	57
1070	2968	51
1100	3257	46

account the porous network morphology. In our samples, the pores are interconnected and, due to the fabrication method of pressing a powder compact in a die, not particularly oriented. From a mechanical point of view, the solid matrix must also be interconnected. Consequently, the assumptions in Landauer's approach are appropriate for the type of the microstructure under study. Experimental results for thermal conductivity have thus been compared with the predictions made with Landauer's expression[15] as well as the Hashin and Shtrikman limits[13].

4. Results and discussion

4.1. Microstructure

Pore volume fractions as a function of the maximum sintering temperature T_{max} are reported in Table 1. The micrograph in Fig. 5 reveals a homogeneous grain size of less than 100 nm and variation in pore shape and size. At least two different characteristic pore sizes can be identified. The mercury porosimetry measurements confirm that the samples exhibit bimodal pore size distributions, constituted by mesopores with diameter less than 50 nm and by macropores with diameter above 50 nm (Fig. 6). The two graphs in Fig. 6 reveal that the mesopore volume fraction increases with the porosity, or in other words when the temperature used for the thermal treatment is lower.

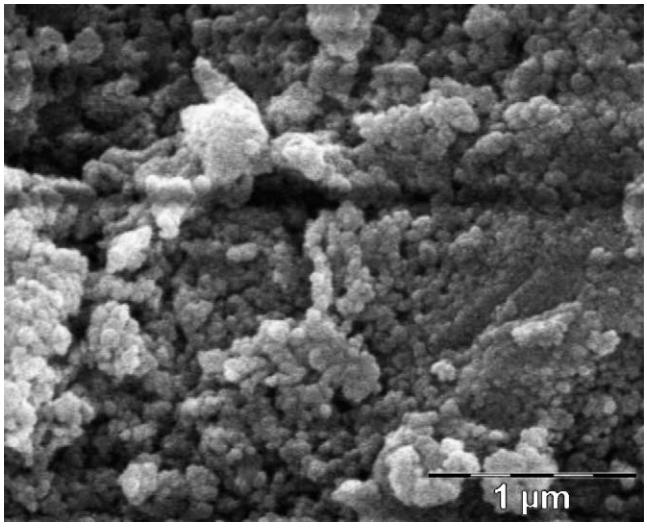

Fig. 5. SEM observation of a fracture of a porous sample, T_{max} = 750 °C.

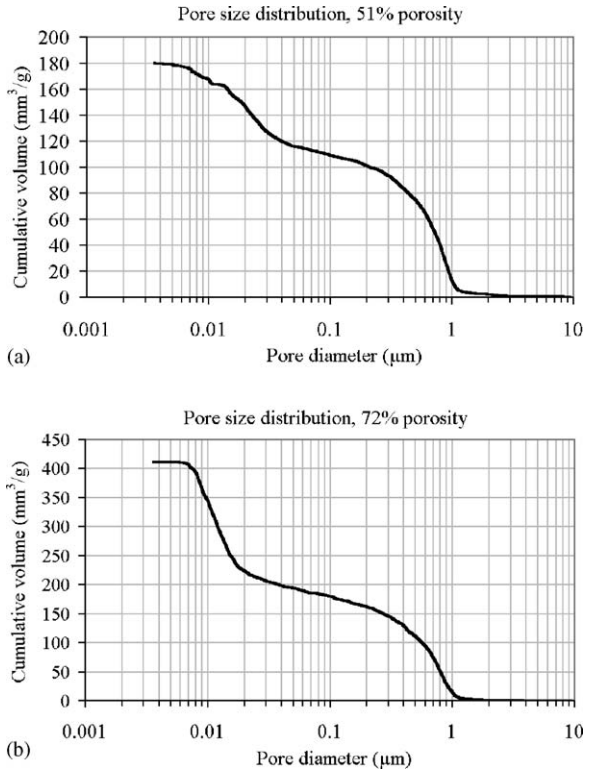

Fig. 6. Pore size distributions for (a) sample containing 51% porosity, T_{max} = 1070 °C; (b) sample containing 72% porosity, T_{max} = 850 °C.

The grain size of the zirconia particles increases from 62 to 70 nm when the applied thermal treatment at 750 °C is replaced by a thermal treatment at 1100 °C. Fully densified samples were also prepared in order to determine the solid phase thermal conductivity. The grain boundaries of a dense sample were revealed by thermal etching and the mean grain size was evaluated to be approximately 4 μm.

4.2. Thermal conductivity study

4.2.1. Thermal transport in zirconia

For monoclinic zirconia[8], the thermal conductivity decreases with temperature which is characteristic of phonon scattering by Umklapp processes. From 300 to 1000 K, this behaviour is close to a $1/T$ dependence. At 25 °C, the thermal conductivity of monoclinic zirconia is approximately 5 W m^{-1} K^{-1}.

The thermal conductivity also decreases strongly with yttria content due to the increased concentration of defects[19,20]. For YSZ, the thermal conductivity behaviour is then similar to that of an amorphous system, in other words almost insensitive to temperature. The thermal conductivities of the Y_2O_3 based monoclinic, tetragonal and cubic ZrO_2 phases were evaluated at 4.2, 3.5 and 2.3 W m^{-1} K^{-1}, respectively[21].

4.2.2. Results

The prediction of the dependence of the effective thermal conductivity with porosity by analytical calculations requires knowledge of the thermal conductivity of each phase. A literature value for the thermal conductivity of air equal to

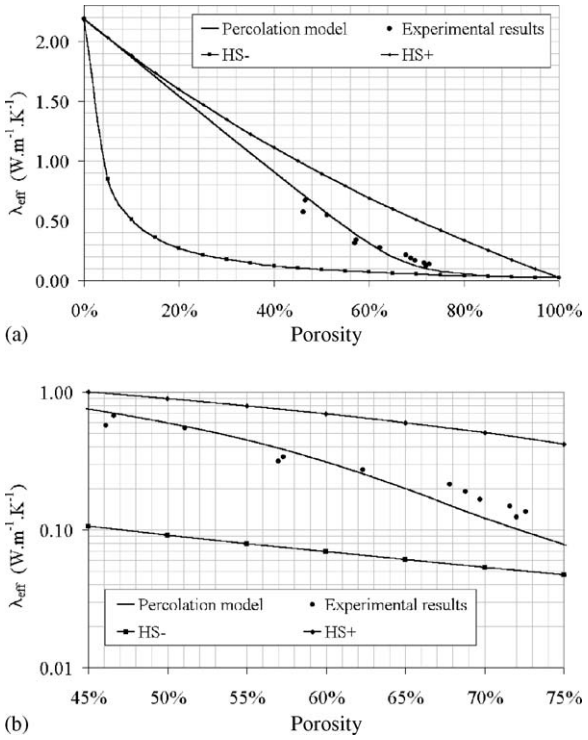

Fig. 7. Effective thermal conductivity as a function of porosity for analytical predictions and experimental measurements. The calculation parameters are: $\lambda_{solid\ phase} = 2.2\ W\ m^{-1}\ K^{-1}$, $\lambda_{air} = 0.026\ W\ m^{-1}\ K^{-1}$. (a) Linear scale, (b) logarithm scale.

$0.026\ W\ m^{-1}\ K^{-1}$ was chosen[22]. An experimental value of $2.2\ W\ m^{-1}\ K^{-1}$, determined for a fully dense sample, was used for the thermal conductivity of the solid phase and this is consistent with literature values for single crystals[20] and polycrystalline zirconia ceramics[8,21]. Fig. 7a shows the measured effective thermal conductivity (λ_{eff}) as a function of pore volume fraction compared with the predictions made from the analytical models. The same information is presented in Fig. 7b with an expanded logarithm scale for the *Y*-axis. The experimental thermal conductivity for the most porous samples approaches a lower limit of $0.1\ W\ m^{-1}\ K^{-1}$. Analytical theory based on isolated inclusions, the Hashin–Shtrikman upper limit, does not yield a good prediction of the effective thermal conductivity for such porous materials. In contrast, experimental results can be seen to agree closely with predictions made with EMPT. We now wish to show how the basic EMPT predicted thermal conductivity—porosity dependence can be modulated by taking into account a more detailed description of the microstructure, especially for porosity exceeding 65%. Three different second order effects are examined.

4.2.3. Adjusting the predictions with the interfacial thermal resistance of the grain boundaries

Porous samples present very small mean grain sizes, less than 70 nm, suggesting that the effect of the interfacial thermal resistance of the grain boundaries should be investigated. Indeed for YSZ, Yang et al.[23] have shown that the interfacial thermal resistance can make a significant contribution to thermal resistance of zirconia ceramics for grain sizes below 100 nm. They evaluated the average interfacial thermal resistance of a grain boundary R_{int} at $0.5 \times 10^{-8}\ m^2\ K\ W^{-1}$. The thermal conductivity of the polycrystalline solid phase is then calculated with the expression[3]:

$$\frac{1}{\lambda_{poly}} = \frac{1}{\lambda_{single\ crystal}} + n \times R_{int} \quad (5)$$

where $\lambda_{single\ crystal}$ is the thermal conductivity of the single crystal and n is the number of interfaces per unit length.

For porous samples, the mean grain size is between 62 and 70 nm. Therefore, using Eq. (5), the previously used value for the solid phase conductivity is reduced by the interfacial thermal resistance of the grain boundaries to $1.9\ W\ m^{-1}\ K^{-1}$ (Table 2). Fig. 8 shows the predicted values of thermal conductivity for porous zirconia ceramics which are calculated using EMPT with this adjusted solid phase value. The correction improves the agreement between experimental values and theory for pore volume fractions below 65%. The effect of the modified solid phase conductivity for porosities above 65% can be neglected as shown by Fig. 8b.

Table 2
Determination of the dense phase thermal conductivity by taking into account the interfacial thermal resistance of the grain boundaries

T_{max} (°C)	Grain size (nm)	$n = \frac{1}{\phi_{grain}}$ (m^{-1})	λ_{poly} ($W\ m^{-1}\ K^{-1}$)
750	62	1.6×10^7	1.9
1100	70	1.4×10^7	1.9

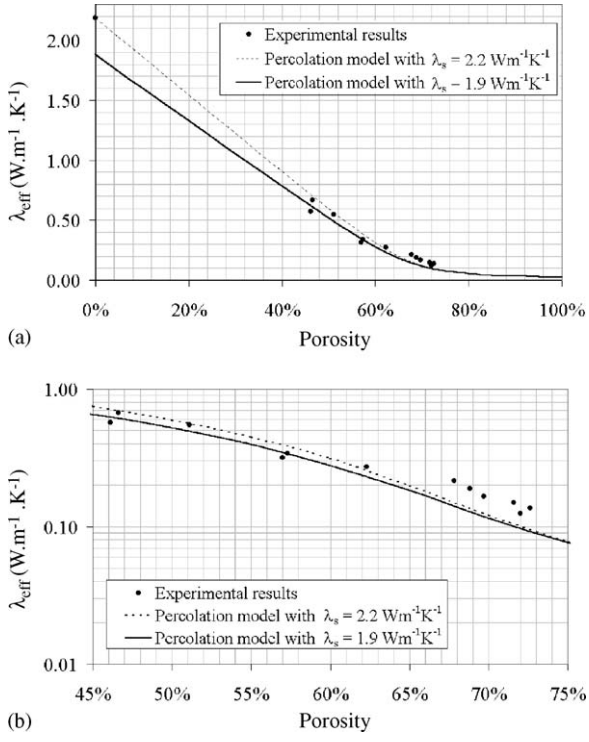

Fig. 8. Thermal conductivity as a function of porosity for experimental measurements and analytical predictions taking into account the grain sizes. (a) Linear scale, (b) logarithm scale.

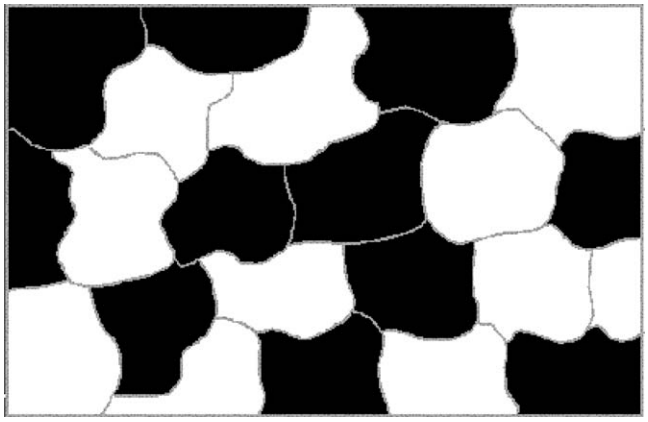

Fig. 9. EMPT considers two phases with a similar size of individual phase regions.

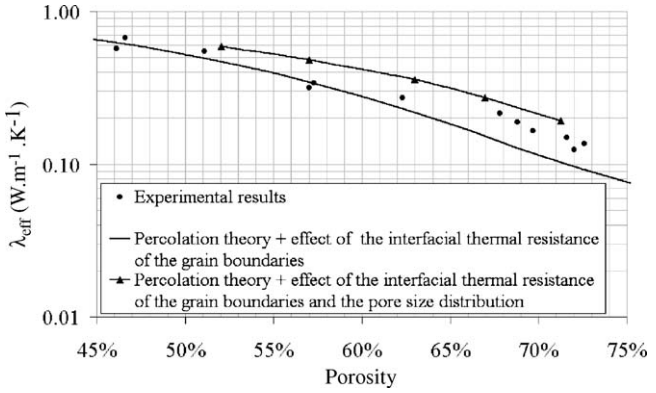

Fig. 11. Thermal conductivity as a function of porosity for experimental measurements and analytical predictions taking into account the average grain size and the bimodal pore size distribution.

4.2.4. Adjusting the predictions with a bimodal pore size distribution

Effective medium percolation theory considers a mixture of two homogeneous phases with a similar size of individual phase regions as shown in Fig. 9. A region of phase 1 should not be surrounded preferentially by either regions of phase 1 or phase 2. Our porous samples are constituted by mesoporous and macroporous networks where the macropores are 100 times larger than the mesopores (Fig. 10a). The previous assumption for the validity of EMPT is not really satisfied. An improvement to the predictions by EMPT can be achieved if we perform a two step calculation as represented in Fig. 10. First the thermal conductivity $\lambda_{solid+mesopore}$ of the mixture constituted by the solid part and the mesoporous network (Fig. 10b) is calculated, using λ_{solid}, λ_{air}, the volumes V_{solid} and $V_{mesopore}$ in $cm^3\,g^{-1}$. Then the effective thermal conductivity is determined using $\lambda_{solid+mesopore}$, λ_{air}, $V_{solid+mesopore}$ and $V_{macropore}$, thus taking into account the macroporous network (Fig. 10c). Obviously, this method requires information on the pore size distribution of the sample to evaluate the respective proportions between V_{solid}, $V_{mesopore}$ and $V_{macropore}$.

Table 3 presents the detailed calculation of the effective thermal conductivity with this two step method using information based on the measured bimodal pore size distribution. The value for the thermal conductivity of the dense solid phase ($1.9\,W\,m^{-1}\,K^{-1}$) takes into account the interfacial thermal resistance of the grain boundaries. The results are plotted in Fig. 11. For a total porosity exceeding 50%, the two step calculation with EMPT increases the values of the effective thermal conductivity, compared to the previous single step method, and these are now closer to the experimental results. We deduce that a bimodal pore size distribution can significantly influence the thermal conductivity of a very porous material. In essence, the packing of pores of different sizes in the solid can lead to a situation where a proportion of then are more isolated in their action of blocking heat flow (i.e. closer to the Maxwell case) then they would be for the equivalent monomodal pore size distribution.

4.2.5. Adjusting the predictions with the pore sizes

Fig. 6 and Table 3 indicate that a high proportion of the porosity in the samples, between 40 and 60% is of very small dimension. We should therefore examine the influence of the pore size on the thermal conductivity of air due to the Knudsen effect[9,24]. The Knudsen number K_n is defined by the expression $K_n = \bar{l}/d$ where $\bar{l}$ is the mean free path of the gas and d is the pore diameter. The gas conductivity λ_{gas} is then related to the Knudsen number and the conductivity at ambient pressure $\lambda_{gas,o}$ in the bulk ($K_n = 0$) by:

$$\lambda_{gas} = \frac{\lambda_{gas,o}}{1 + 2\beta K_n} \tag{6}$$

where β is a coefficient equal to 1.5 for air. At atmospheric pressure, $\lambda_{air,o} = 0.026\,W\,m^{-1}\,K^{-1}$. A plot of Eq. (4) reveals a

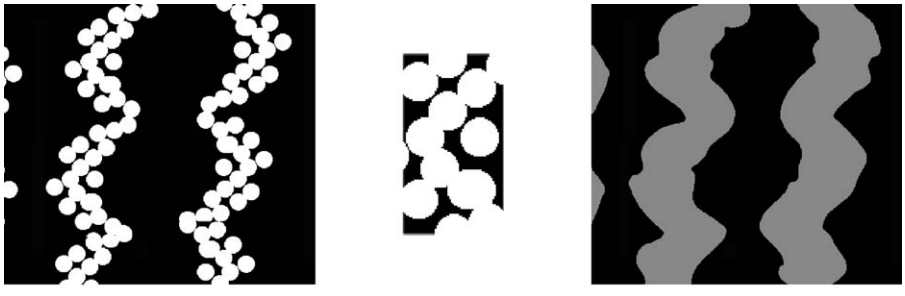

Fig. 10. Two step calculation of the effective thermal conductivity by EMPT. (a) Solid (white), mesoporous and macroporous networks. (b) Solid and mesopores, step 1: $\lambda_{solid+mesopore}$. (c) Solid + mesopores in grey and macropores, step 2: λ_{eff}.

Table 3
Calculation of the effective thermal conductivity using the two step EMPT model to take into account the bimodal pore size distribution

Porosity (%)	$\frac{V_{mesopore}}{V_{mesopore}+V_{solid}}$	$\lambda_{solid+mesopore}$ (W m^{-1} K^{-1})	$\frac{V_{macropore}}{V_{macropore}+V_{mesopore}+V_{solid}}$	λ_{eff} (W m^{-1} K^{-1})
72	0.59	0.32	0.30	0.19
68	0.53	0.46	0.30	0.27
62	0.46	0.63	0.31	0.36
57	0.38	0.86	0.31	0.48
51	0.30	1.08	0.32	0.59

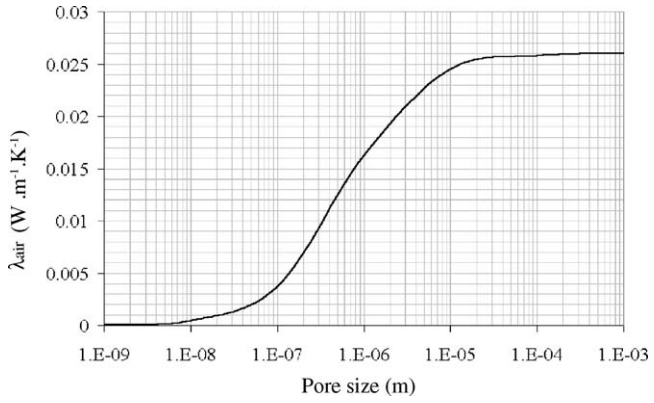

Fig. 12. Effective thermal conductivity of pores, containing air, as a function of pore size (Knudsen effect).

significant decrease in the effective thermal conductivity of a pore, containing air, when its size is below 10 μm (Fig. 12). This information is now used to readjust the previous calculations. The value calculated for $d = 10$ nm is used for the pore volume fraction corresponding to pores with diameter less than 50 nm (mesopores). The value obtained for $d = 1$ μm is assigned to the volume fraction of the macropores.

These final values calculated with EMPT, taking into account the interfacial thermal resistance of the grain boundaries, the bimodal pore size distribution and the Knudsen effect are compared with experimental results in Fig. 13. The calculated curve exhibits significantly lower thermal conductivity for total pore volume fractions exceeding 65% and provides a satisfactory agreement to experimental values in this range of porosity.

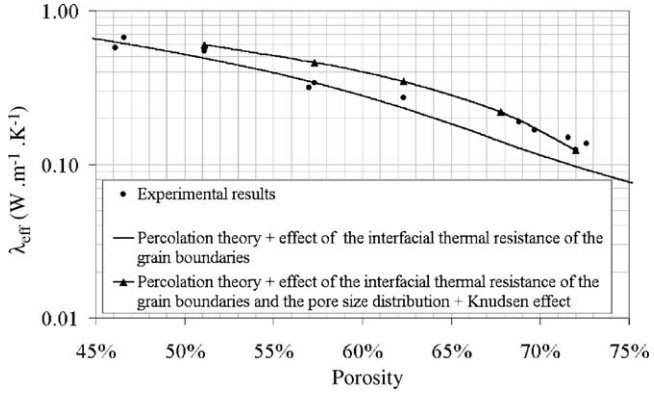

Fig. 13. Thermal conductivity as a function of porosity for experimental measurements and analytical predictions taking into account the average grain size, the pore size distribution and the Knudsen effect.

5. Conclusion

Yttria stabilised zirconia ceramics with pore volume fractions from 45 to 75% were prepared and characterised with respect to their thermal conductivity. The thermal conductivity of the most porous samples approaches a lower limit of 0.1 W m^{-1} K^{-1}. Experimental results were compared to chosen analytical models and are shown to agree closely with predictions made by effective medium percolation theory for a two-phase system. This agreement was improved even further by corrections based on detailed microstructural information. The strong interest of our approach is to show how each of the factors considered can have a significant effect on the thermal conductivity, though not necessarily for the total range of pore volume fractions.

First, the interfacial thermal resistance of the grain boundaries reduces the thermal conductivity of the solid phase by 14% from 2.2 to 1.9 W m^{-1} K^{-1}. Second, the agreement was improved for porosities above 65% by applying the EMPT calculation in two steps taking into account the bimodal pore size distribution and also the dependence of the thermal conductivity of air with the pore size due to the Knudsen effect. We conclude that for obtaining a very thermally insulating material, the microstructure should exhibit a high volume fraction of pores which are as small as possible. Finally, a monomodal pore size distribution is shown to be more effective for obtaining low thermal conductivity in our porous zirconia ceramics than a bimodal pore size distribution which, in fact, yields a less continuous nature to the heat blocking pore phase.

References

1. Schulle, W. and Schlegel, E., Fundamentals and Properties of Refractory Thermal Insulating Materials (High-Temperature Insulating Materials). *Ceramic Monographs—Handbook of Ceramics, Supplement to Interceram, Vol 40[7]*, No. 2.6.3., 1991, pp. 1–12.
2. ECFIA Action, European Ceramic Fibre Industries Association, 3 rue du colonel Moll. 75017 Paris, France, Information Sheets Nos. 2 and 3, March 1999.
3. Smith, D. S., Fayette, S., Grandjean, S., Martin, C., Telle, R. and Tonnessen, T., Thermal resistance of grain boundaries in alumina ceramics and refractories. *J. Am. Ceram. Soc.*, 2003, **86**, 105–111.
4. Bucko, M. M. and Haberko, K., Crystallization of zirconia under hydrothermal conditions. *J. Am. Ceram. Soc.*, 1995, **78**, 3397–3400.
5. Scott, H. G., Phase relationships in the zirconia–yttria system. *J. Mater. Sci.*, 1975, **10**, 1527–1535.
6. Parker, W. J., Flash method of determining thermal diffusivity, heat capacity and thermal conductivity. *J. Appl. Phys.*, 1961, **32**, 1679–1684.
7. Degiovanni, A., Diffusivité et méthode Flash. *Rev. Gén. Therm. (France)*, 1977, **185**, 420–441.

8. Raghavan, S., Wang, H., Dinwiddie, R. B. and Porter, W. D., The effect of grain size, porosity and yttria content on the thermal conductivity of nanocrystalline zirconia. *Scripta Materialia*, 1998, **39**, 1119–1125.
9. Collishaw, P. G. and Evans, J. R. G., An assessment of expressions for the apparent thermal conductivity of cellular materials. *J. Mater. Sci.*, 1994, **29**, 2261–2273.
10. Maxwell, J. C., *A Treatise on Electricity and Magnetism, Vol 1*, Clarendon Press, Oxford, 1892, p. 440.
11. Rayleigh, L., On the influence of obstacles arranged in rectangular order upon the properties of medium. *Phil. Mag.*, 1892, **34**, 481–507.
12. Russel, H. W., Principle of heat flow in porous insulators. *J. Am. Ceram. Soc.*, 1935, **18**, 1–5.
13. Hashin, Z. and Shtrikman, S., A variational approach to the theory of the effective magnetic permeability of multiphase materials. *J. Appl. Phys.*, 1962, **33**, 3125–3131.
14. Bruggeman, D. A. G., Berechnung verschiedener physikalischer Konstanten von heterogenen Substanzen. I.: Dielektrizitätskonstanten uns Leitfähigkeiten der Mischkörper aus isotropen Substanzen. *Ann. Der Physik.*, 1935, **5**, 636–664.
15. Landauer, R., The electrical resistance of binary metallic mixtures. *J. Appl. Phys.*, 1952, **21**, 779–784.
16. Ast, D. G., Evidence for percolation-controlled conductivity in amorphous As_xTe_{1-x} films. *Physical Review Letters*, 1974, **33**, 1042–1045.
17. Schulz, B., Thermal conductivity of porous and highly porous materials. *High Temperatures–High Pressures*, 1981, **13**, 649–660.
18. Bjorneklett, A., Haukeland, L., Wigren, J. and Kristiansen, H., Effective medium theory and the thermal conductivity of plasma-sprayed ceramic coatings. *J. Mater. Sci.*, 1994, **29**, 4043–4050.
19. Schelling, P. K. and Phillpot, S. R., Mechanism of thermal transport in zirconia and yttria-stabilized zirconia by molecular-dynamics simulation. *J. Am. Ceram. Soc.*, 2001, **84**, 2997–3007.
20. Bisson, J.-F., Fournier, D., Poulain, M., Lavigne, O. and Mévrel, R., Thermal conductivity of yttria-zirconia single crystals, determined with spatially resolved infrared thermography. *J. Am. Ceram. Soc.*, 2000, **83**(8), 1993–1998.
21. Hasselman, D. P. H., Johnson, L. F., Bentsen, L. D., Syed, R. and Lee, H. L., Thermal diffusivity and conductivity of dense polycrystalline ZrO_2 ceramics: a survey. *Am. Ceram. Soc. Bull.*, 1987, **66**, 799–806.
22. Weast, R. C., ed., *Handbook of Chemistry and Physics*. 55th ed. CRC Press, Cleveland, Ohio, 1974, p. E2.
23. Yang, H. S., Bai, G. R., Thompson, L. J. and Eastman, J. A., Interfacial thermal resistance in nanocrystalline yttria stabilised zirconia. *Acta Materialia*, 2002, **50**, 2309–2317.
24. Litovsky, E., Shapiro, M. and Shavit, A., Gas pressure and temperature dependances of thermal conductivity of porous materials. Part 2. Refractories and ceramics with porosity exceeding 30%. *J. Am. Ceram. Soc.*, 1996, **79**, 1366–1376.